Structure and enzymatic degradation of the polysaccharide secreted by Nostoc commune

Sophie Drouillard, Laurent Poulet, Eric Marechal, Alberto Amato, Laurine Buon, Mélanie Loiodice, William Helbert

Structure and enzymatic degradation of the polysaccharide secreted by *Nostoc commune*

Sophie Drouillard[1], Laurent Poulet[1], Eric Marechal[2], Alberto Amato[2], Laurine Buon[1], Mélanie Loiodice[1], William Helbert[1*]

[1] CERMAV, CNRS and Grenoble Alpes Université, BP53, 38000 Grenoble Cedex 9, France

[2] Laboratoire de Physiologie Cellulaire Végétale, Université Grenoble Alpes, CEA, CNRS, INRAE, IRIG-LPCV, 38054 Grenoble Cedex 9, France

Abstract

Noctoc commune is a cyanobacterium living in various and extreme environments. Its ability to survive in desert, on ice or high altitude is explained by its exceptional metabolism and its capacity to resist to desiccation. *N. commune* cells are embedded in a gelatinous matrix made of polysaccharides which fixes water and participates in maintaining the cells in hydrated conditions. The structure of the polysaccharide of *N. commune* harvested in Saint Martin d'Uriage (France) and the oligosaccharides obtained after its enzymatic degradation were determined. The repeating unit of the main chain is a tetra-saccharide: [→4)-β-D-Glc*p*-(1→4)-β-D-Xyl*p*-(1→4)-β-D-Glc*p*-(1→4)-α-D-Gal*p*-(1→], branched at position 6 of a glucose residue by a β-linked pyruvated glucuronic acid residue. About 30% of the Xyl*p* residues were branched with a Xyl*f* residue. Comparison of this structure with the polysaccharides secreted by other *Nostoc* species and strains suggest a strong selection pressure on the structure in agreement with its important biological role.

Keywords: *Nostoc commune*; Polysaccharide structure; NMR; Enzymatic degradation

1. Introduction

The *Nostoc* genus groups very diverse species of filamentous cyanobacteria that form microscopic or macroscopic colonies embedded in a gelatinous matrix. The colonies may adopt various morphologies: sheet-like (*N. commune*), hair-like (*N. flagelliform*) or spheric morphology (*N. pruniform*, *N. sphaeroides*) as a function of the species and their growth conditions. *Nostoc sp*. have been collected and used for food and medicine for centuries in many places in the world. Currently, *Nostoc flagelliform* ("facai") in China and *Nostoc pruniform* ("llullucha") in South America are nowadays probably the most used for their nutritive properties as diet complement (Dodds & Gudder, 1995; Gao, 1998; Qui, Liu J., Liu Z.& Liu S., 2002; Sand-Jensens, 2014). These microorganisms may be found in various and extreme, terrestrial and aquatic environments. They tolerate the freezing temperature of Antarctic (e.g. *Nostoc commune*) (Davey, 1989; Novis et al., 2007), high temperature of desert (e.g. *Nostoc flagelliform*; Gao, 1998, Hu, Liu, Paulsen, Petersen & Klaveness, 2003) and sun radiation found in the altitude of Andes (Fleming & Prufert-Bebout, 2010). The exceptional capacity of *Nostoc spp*. to live in poor habitat and to adapt to extreme environments is explained by their metabolisms and their capacity to resist to desiccation (Dodds & Gudder, 1995; Sand-Jensen, 2014). As other cyanobacteria, *Nostoc spp*. can fix carbon by photosynthesis and they developed strategies to incorporate atmospheric nitrogen. To face desiccation, cyanobacterial cells differentiate into akinete cells (resting-state cells of cyanobacteria) which germinate when conditions become more favorable (Perez, Forchhammer, Salerno & and Maldener, 2016).

The gelatinous matrix embedding the cyanobacterial colonies is mainly composed of a high molecular weight polysaccharide forming a highly viscous solution. The physicochemical properties of the polysaccharide and its capacity to retain water is correlated to the structural properties of the macromolecule. Composition analyses of the secreted polysaccharide conducted on numerous species and strains of *Nostoc* revealed that some neutral monosaccharide residues (glucose: Glc; galactose: Gal; xylose: Xyl) and uronic residues (glucuronic acid:GlcA) are very often present. Other pentose residues such as arabinose (Ara) and ribose (Rib), and organic groups (lactate, pyruvate) also found in the composition increase the complexity of the polysaccharides (Huang, Liu, Paulsen& Klaveness, 1998; Brüll et al., 2000; Pereira et al., 2009).

The first structure of the polysaccharides secreted by two strains of *Nostoc commune* collected in Asia were determined by Helm and co-workers (2000) and Brüll and co-workers (2000). The structures showed a similar tetrasaccharide repeating unit of the main chain made of [→4) β-D-Glc (1→4) α-D-Gal (1→4) β-D-Glc (1→4) Xyl (1→] carrying an uronic residue (glucuronic acid: GlcA, or nosturonic acid: pyruvated-GlcA) and a deoxy residue (Ara, Rib). The structure of the polysaccharides, and more especially the decoration of the main chain, was found to change with growth conditions (Brüll et al., 2000).

The exact biological role of the matrix polysaccharide is not well understood but it probably participate in the survival of *Nostoc spp*. by retaining water in dry environment and by participating in the rewetting of the akinete cells prior they germinate when environmental conditions are favorable. Assuming that the biological role in the survival of *Nostoc* cells is driven by the structural features of the macromolecules, we hypothesized that their chemical characteristics were probably conserved in the *Nostoc commune* species and may be shared with other species of the genus *Nostoc*. In this context, we have analyzed the polysaccharide structure of a strain of *Nostoc commune* collected in Europe. With the help an enzyme catalyzing the degradation of the *Nostoc commune* polysaccharides, recently identified through the systematic screening of distantly related carbohydrate active enzymes (Helbert et al. 2019), we have produced a series of oligosaccharides helping in the resolution of the chemical structure of the polysaccharide.

2. Material and methods

2.1. DNA extraction

Frozen sheet-like *Nostoc commune* were grinded to fine powder in liquid nitrogen. The sample was suspended in 500µl of lysis buffer (250 mM Tris pH 8.2, 100 mM EDTA, 2% SDS, 100 mM NaCl) and was warmed for 30 minutes at 90°C. During this step, the suspension was vortexed for 30 seconds every 10 minutes. Then, 500 µL of phenol:chloroform:isoamyl alcohol (25:24:1) were added to the sample and mixed vigorously to obtain a homogeneous suspension (at least 3 minutes with vortex). In order to separate the cell debris and the aqueous solution containing the nucleic acids, the samples were centrifuged 10 minutes at 17,000 × g at 4°C. The upper phase was transferred to a new tube and 300 µL of chloroform:isoamyl alcohol (24:1) were added. The sample was vigorously mixed by inverting the tubes followed by centrifugation for 10 min at 13,000 × g at 4°C aiming at separating the two phases. The upper aqueous phase was transferred in a new tube and 30µL of 3M Na-acetate and 1.5 volumes (750 µL) of absolute ethanol were added to precipitate the DNA. Precipitation was conducted for at least 20 minutes at -20°C. DNA salts were pelleted by centrifugation (10 min. at 13,000 × g at 4°C). The supernatant was discarded and the pellet was washed twice with 500 µL of 70% ethanol. Washing steps were done by adding ethanol to the pellet and centrifuging 5 minutes at 13,000 × g at 4°C. After the second ethanol washing, the supernatant was carefully removed without disturbing the pellet and it was air dried for 30-60 minutes. The pellet was then resuspended in TE buffer. Purity and quantity were controlled with a NanoDrop spectrophotometer.

2.2. PCR amplification and sequencing

100 ng of the purified DNA was used as template for PCR amplification. CYA359F and CYA781R (Boutte, Grubisic, Balthasart & Wilmotte, 2006) primer pair was used to amplify a 427nt

fragment of the 16S rRNA gene. The PCR reactions were performed in 25 µL total volume, containing 5 µl 5X Phusion HF buffer, 200 µM (final concentration) dNTPs, 0.5 µM of each primer, 0.5 units of BioLabs Phusion® High-Fidelity DNA Polymerase (M0530). A Biorad T100™ Thermal Cycler was used for PCR reactions with the following cycles: a desaturation step at 98°C for 30 seconds, a gradient from 45 to 60 °C for the annealing (5 temperatures) and an elongation of 15 seconds at 72°C. The PCR products were loaded on a 0.8% agarose TAE gel electrophoresis working for 30 minutes at 100V. The DNA fragment was visualized on a UV/white light transilluminator. All the tested annealing temperatures produced an amplification with a clear band at the expected size. Because no band of no specific amplification was observed on the gel, PCR products were purified using a Macherey-Nagel NucleoSpin® Gel and PCR Clean-up kit following the manufacturer's instructions. Purified PCR products were sent out to Eurofins Genomics for sequencing in both 5' and 3' directions using the amplification primers. Sequences were visualized and assembled in BioEdit Sequence Alignment Editor (Hall, 1999) and blasted against GenBank. All the top hit sequences were downloaded and further analyzed.

2.3. Polysaccharide extraction and purification

Small pieces of *Nostoc commune* were suspended in distilled water at 100°C for 1h. After removing the water and rinsing twice the *N. commune* fragments with fresh water, the sample was treated at 70°C for 6 h by a bleaching solution which consisted of 1 volume of 1.7% aqueous $NaClO_2$ and 1 volume of acetate buffer (pH 4.9), completed with 3 volumes of distilled water. The sample was washed with distilled water by repeated centrifugation and finally resuspended in 3% (w/v) KOH solution overnight at room temperature. The insoluble fraction was discarded by centrifugation. The polysaccharide was precipitated by adding an equal volume of ethanol to the supernatant. The pellet was washed by repeated centrifugation with water/ethanol solution (1/1, v/v). The polysaccharide was finally suspended in water and lyophilized.

2.4. Monosaccharide analysis

The molar ratio of the monosaccharides was determined according to (Kamerling, Gerwig, Vliegenthart & Clamp, 1975) modified by (Montreuil et al., 1986). The EPS was hydrolysed with 3 M MeOH/HCl at 110°C for 4 h, followed by re-N-acetylation with Ac_2O overnight at room temperature. The methyl glycosides were converted to their corresponding trimethylsilyl derivatives. Separation and quantification of the per-*O*-trimethylsilyl methyl glycosides were performed using gas-liquid chromatography (GLC) on an Agilent system equipped with a HP-5 ms capillary column (Agilent 0.25 mm x 30 m). The trimethylsilyl derivatives were analysed using the following temperature program: 120°C→180°C at 3°C/min, 180°C→200°C at 2°C/min, 200°C for 5 min.

2.5. Methylation analysis

Glycosyl linkage positions were determined as described in (Hakomori, 1964). Hydroxyl groups were methylated using the lithium dimethylsulfonyl as the anion and methyl iodide in Me_2SO (Blakeney and Stone, 1985; Kvernheim, 1987). After two methylation steps, the permethylated products was carboxyl-reduced by LiBD4 in absolute ethanol for 2h at 80°C (Linnerborg and al, 1997). Excess of borodeuteride was decomposed with 10% acetic acid. After evaporation, the permethylated and carboxyl-reduced products were hydrolysed in 2M trifluoroacetic acid (TFA) for 2h at 120°C, then reduced with $NaBD_4$ in an NH_4OH solution for 30min at 80°C, and finally acetylated with 200µL of 1-methyl imidazole and 2mL acetic anhydride for 10min at room temperature. GC-mass spectrometry (MS) was performed on an Agilent instrument fitted with a Supelco SP2380 capillary column (0.25 mm× 30 m). The temperature program was 150 °C for 2 min, 150 °C → 240 °C at 3 °C/min, 240 °C for 5 min. Ionisation was carried out in electron impact mode (EI, 70 eV). All analyses were conducted in triplicate.

2.6. Preparation of the *Nostoc* polysaccharide hydrolase

Nostoc polysaccharide hydrolase was overexpressed and purified by affinity chromatography as previously reported in Helbert and co-workers (2019). Briefly, the gene encoding the enzymes was cloned in pHTP1 (NZYtech, Portugal) vector harboring a His_6-tag at the N-terminal position. The enzyme was overexpressed in *E. coli* BL21(DE3) pLysS strain grown in NZY auto-induction LB media (NZYtech, Portugal). After a freeze-thaw cycle, the protein was purified by affinity using a nickel agarose affinity resin (Ni-NTA resin, Qiagen) loaded on poly-prep® chromatography columns (Bio-Rad 731-1550). The His_6-tagged recombinant enzyme was eluted with increasing amounts of imidazole (20 mM, 50 mM, 150 mM, 300 mM and 500 mM). The purity of the fractions was estimated by 10% SDS-PAGE analysis.

2.7. Enzymatic degradation and purification of oligosaccharides

Enzymatic degradations were carried out by incubating 10 mL of purified polysaccharides (1% w/v in 20 mM Tris-HCl pH 7.5, 20 mM NaCl) with 500 µL of purified enzyme ($0.60 µg.µL^{-1}$) at 25°C. End-products were purified on a semi-preparative size-exclusion chromatography system which consisted of a Knauer pump (pump model 100), a HW40 Toyopearl column (120 x 16 mm; Tosoh Corporation), a refractive index detector (Iota 2, Precision Instruments) and a fraction collector (Foxy R, Teledyne Isco 1) mounted in series. Elution was conducted at a flow rate of 0.4 mL/min at room temperature using 100 mM $(NH_4)_2CO_3$ as the eluent. The fractions containing the oligosaccharides were collected and freeze-dried.

2.8. NMR

Carbon-13 and proton NMR spectra were recorded with a Bruker Avance 400 spectrometer operating at a frequency of 100.618 MHz for ^{13}C and 400.13 MHz for ^{1}H. Samples were solubilized in D_2O at a temperature of 293 K for the oligosaccharides and 353 K for the polysaccharide. Residual signal of the

solvent was used as internal standard: HOD at 4.85 ppm at 293 K and 4.25 at 353 K. ^{13}C spectra were recorded using 90° pulses, 20,000 Hz spectral width, 65,536 data points, 1.638 s acquisition time, 1 s relaxation delay and between 8192 and 16,834 scans. Proton spectra were recorded with a 4006 Hz spectral width, 32,768 data points, 4.089 s acquisition times, 0.1 s relaxation delays and 16 scans. The ^{1}H and ^{13}C-NMR assignments were based on ^{1}H-^{1}H homonuclear and ^{1}H-^{13}C heteronuclear correlation experiments (correlation spectroscopy, COSY; heteronuclear multiple-bond correlation, HMBC; heteronuclear single quantum correlation, HSQC). They were performed with a 4006 Hz spectral width, 2048 data points, 0.255 s acquisition time, 1 s relaxation delay; 32 to 512 scans were accumulated.

3. Results and discussion

3.1 Identification of the *Nostoc commune* strain

The *Nostoc commune* strain was collected at Saint Martin d'Uriage (France, 45°09'53.7"N 5°51'18.9"E). The macroscopic colonies have dark green gelatinous sheet-like morphology. After extraction, 16S RNA was sequenced and compared with *Nostoc* 16S RNA sequences available in Genebank. The sequence showed >98% identity with *Nostoc commune* strains isolated in Europe (AB113665.1, France; AY577536.1, Czech Republic, strain EV1-KK1; KY283050.1, Russia, strain ACSSI 030), Asia (AB933330.2, Japan, strain KU006; EU178142.1, China, strain AHNG0605; KY129708.1, India, strain BHU81) and North America (HQ877826.1, Mexico, strain 257-16). The 16S RNA analyses demonstrated that the cyanobacterial colonies collected share the same molecular characteristic of *Nostoc commune* strains.

Table 1. Methylation analysis of the matrix polysaccharide secreted by *Nostoc commune*. The percentage of the main linkages observed were estimated by measuring the surface area of the signal.

Residue	Partially Methylated Alditol Acetate	Deduced Linkage	Peak surface area (%)
Glucose	1,4,5-Tri-O-acetyl-1-deuterio-2,3,6,-tri-O-methyl-D-glucitol	→4)-Glc*p*-(1→	22.7
Glucose	1,4,5,6-Tetra-O-acetyl-1-deuterio-2,3,-di-O-methyl-D-glucitol	→4,6)-Glc*p*-(1→	24.1
Xylose	1,3,4,5-Tetra-O-acetyl-1-deuterio-2-O-methyl-D-xylitol	→3,4)-Xyl*p*-(1→	7.7
Xylose	1,4,5-Tri-O-acetyl-1-deuterio-2,3 di-O-methyl-D-xylitol	→4)-Xyl*p*-(1→	8.8
Xylose	1,4-Di-O-acetyl-1-deuterio-2,3,5-tri-O-methyl-D-xylitol	Xyl*f*-(1→	1.8
Galactose	1,4,5-Tri-O-acetyl-1-deuterio-2,3,6-tri-O-methyl-D-galactitol	→4)-Gal*p*-(1→	18.1
Glucuronic acid	1,5,6-Tri-O-acetyl-1,6,6-trideuterio-2,3,4-tri-O-methyl-D-glucitol	GlcA*p*-(1→	1.5

3.2 Characterization of the matrix polysaccharide of *Nostoc commune*

Composition analysis using gas chromatography, after the complete hydrolysis of the polysaccharide and trimethylsilyl derivatization of the products, revealed glucose (Glc), galactose (Gal), xylose (Xyl) and glucuronic acid (GlcA) (% molar ratio Glc/Gal/Xyl/GlcA 1/0.48/0.90/0.14) (Figure S1).

Traces of mannose (% molar ratio Glc/Man 1/0.08) were also detected in the purified polysaccharide. Methylation analyses (Table 1) revealed that the Glc*p* residues is mainly involved in 1,4- and 1,4,6-linkages; the Gal*p* residue participate in 1,4 linkages and the Xyl*p* residue is bound by the position 1, 3 and 4. Terminal Glc*p*A was also observed suggesting its branching on the main chain. In addition, we detected a derivative presenting the same elution time than the 1,4-di-O-acetyl-1-deuterio-2,3,5-tri-O-methyl-D-xylitol (Figure S2A) which is present in low amount in the xylose standard (Figure S2B). The fragmentation products of the derivatives were compared (Figure S3) and validated the occurrence of a terminal xylofuranoside (T-Xyl*f*) involved in a side chain.

Carbon and proton NMR recorded on the polymer revealed the occurrence of six different residues as illustrated by the heteronuclear $^{1}H/^{13}C$ chemical shift correlation (HSQC) presented in Figure 1. The proton correlation systems observed in the homonuclear $^{1}H/^{1}H$ chemical shift correlation (COSY, TOCSY), the determination of the chemical shifts and coupling constants (Table 2) confirmed the occurrence of glucose, galactose, glucuronic acid and xylose residues expected from chemical analyses.

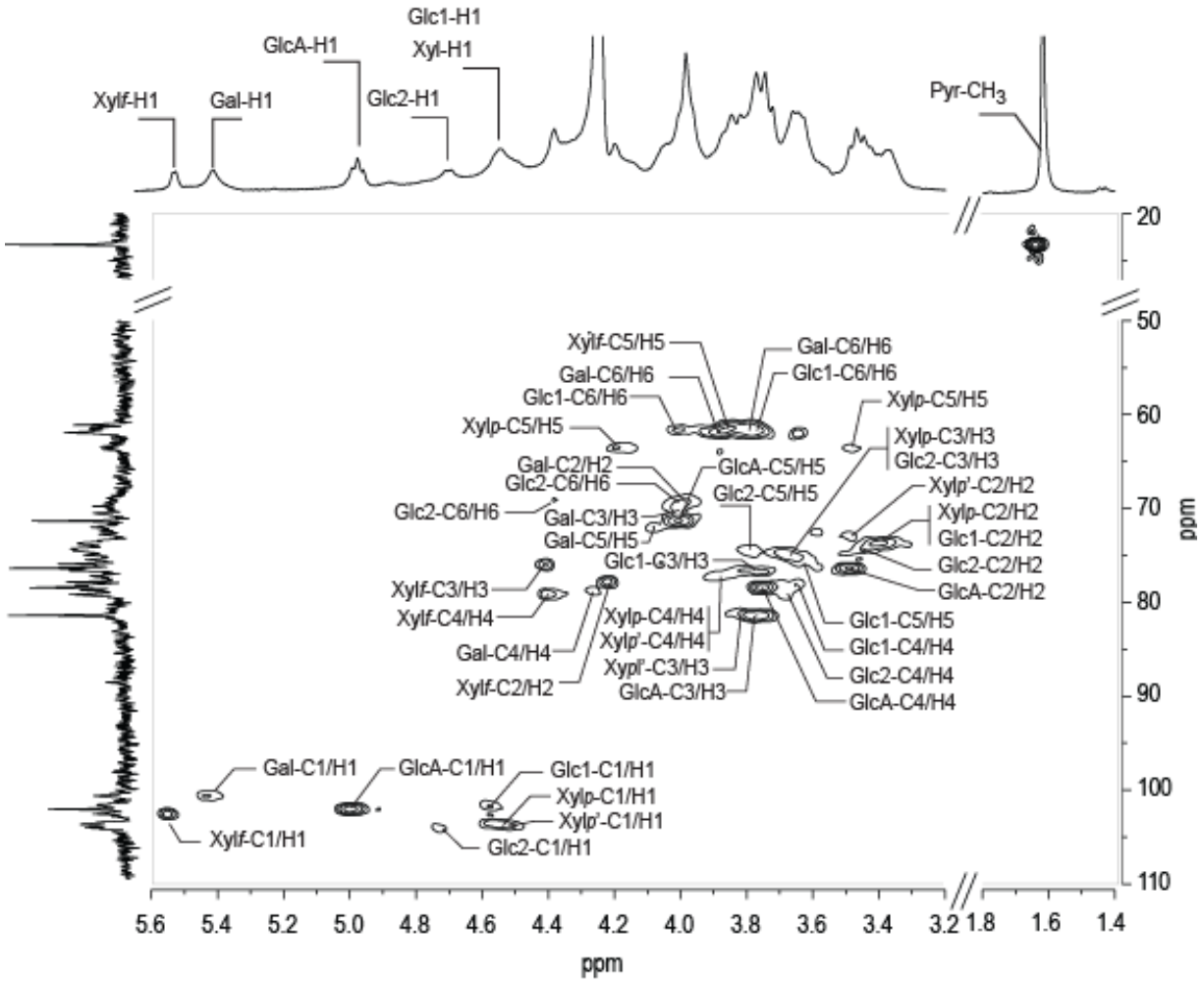

Figure 1. Heteronuclear $^{1}H/^{13}C$ chemical shift correlation (HSQC) spectrum of the polysaccharide secreted by *Nostoc commune*. The spectrum was recorded at 353 K

Two glucose residues could be distinguished in the spectra (Glc1-C1/H1: 100.90/4.57 ppm and Glc2-C1/H1: 103.33/4.71 ppm), one galactose residue (Gal-C1/H1: 99.91/5.42 ppm) and three xylose residues were observed: two in pyrano configuration (Xyl*p*-C1/H1: 102.97/4.49 ppm and Xyl'p-C1/H1: 102.75/4.54 ppm) and one in furano configuration (Xyl*f*-C1/H1: 101.86/5.54 ppm). The glucuronic acid residue (GlcA-C1/H1: 101.34/4.99 ppm) was systematically decorated by a pyruvate group which could be removed by a mild acid treatment conducting to the shift of the anomeric proton from 4.99 to 4.57 ppm (Figure S4). Investigations of the linkages using heteronuclear $^{1}H/^{13}C$ chemical shift correlation (HMBC) revealed strong similarities with the previous work of Helm and co-workers (2000) on the polysaccharides of *N. commune* DRH-1. The repeating unit seemed very similar except that the glucuronic residue was decorated by a pyruvate group instead of lactate (named nosturonic residue) and that the ribofuranoside residue was replaced by a xylofuranoside residue.

Table 2: ^{1}H and ^{13}C NMR chemical shifts recorded on the secreted polysaccharide of *Nostoc commune*.

Sugar Residue		1	2	3	4	5	6 (6a,6b)	Pyr (CH_3, C, CO)
Polymer								
Glc-1 →4)-β-D-Glc*p*-(1→+	^{1}H	4.57	3.39	3.78	3.65	3.58	3.98, 3.78	
	^{13}C	100.90	72.97	76.00	76.87	74.91	60.74	
Xyl*p* →4)-β-D-Xyl*p*-(1→	^{1}H	4.49	3.40	3.65	3.86	4.17, 3.47		
	^{13}C	102.97	73.00	73.74	76.01	63.00		
Glc-2 →4,6)-β-D-Glc*p*-(1→	^{1}H	4.71	3.43	3.66	3.68	3.78	4.34, 4.00	
	^{13}C	103.33	73.56	74.07	78.07	73.56	69.09	
Pyr-GlcA β-D-(2,3Pyr)-Glc*p*A (1→	^{1}H	4.99	3.48	3.76	3.74	4.00	no	1.64
	^{13}C	101.34	75.61	80.70	77.95	70.64	174.90	22.59, 109.03, 175.65
Gal →4)-α-D-Gal*p*-(1→	^{1}H	5.42	4.00	4.01	4.27	4.06	3.87, 3.77	
	^{13}C	99.91	69.02	69.79	78.07	71.30	61.22	
Xyl*p*' →3,4)-β-D-Xyl*p*-(1→	^{1}H	4.54	3.48	3.80	3.88	4.17, 3.47		
	^{13}C	102.75	71.77	79.87	76.01	62.70		
Xyl*f* α-D-Xyl*f*-(1→	^{1}H	5.54	4.21	4.40	4.39	3.82		
	^{13}C	101.86	77.13	75.22	78.46	60.40		
Depyruvated Polymer								
dPyr β-D-Glc*p*A-(1→	^{1}H	4.57	3.42	3.58	3.58	3.77	no	
	^{13}C	102.63	72.83	75.45	71.71	76.18	175.75	

3.3 Analyses of the enzymatic degradation products of the *N. commune* polysaccharide

To deepen the structural characterization of the polysaccharide, we took advantage of our recent discovery of an endo-acting enzyme able to cleave the polysaccharides in oligosaccharides (Helbert et al., 2019). This new enzyme which is the first member of the glycoside hydrolase family GH160 to cleave the

linkage between the galactose (sub-site -1) and a glucose (sub-site +1) residues giving oligosaccharide series with galactose at the reducing end and glucose at the non-reducing end.

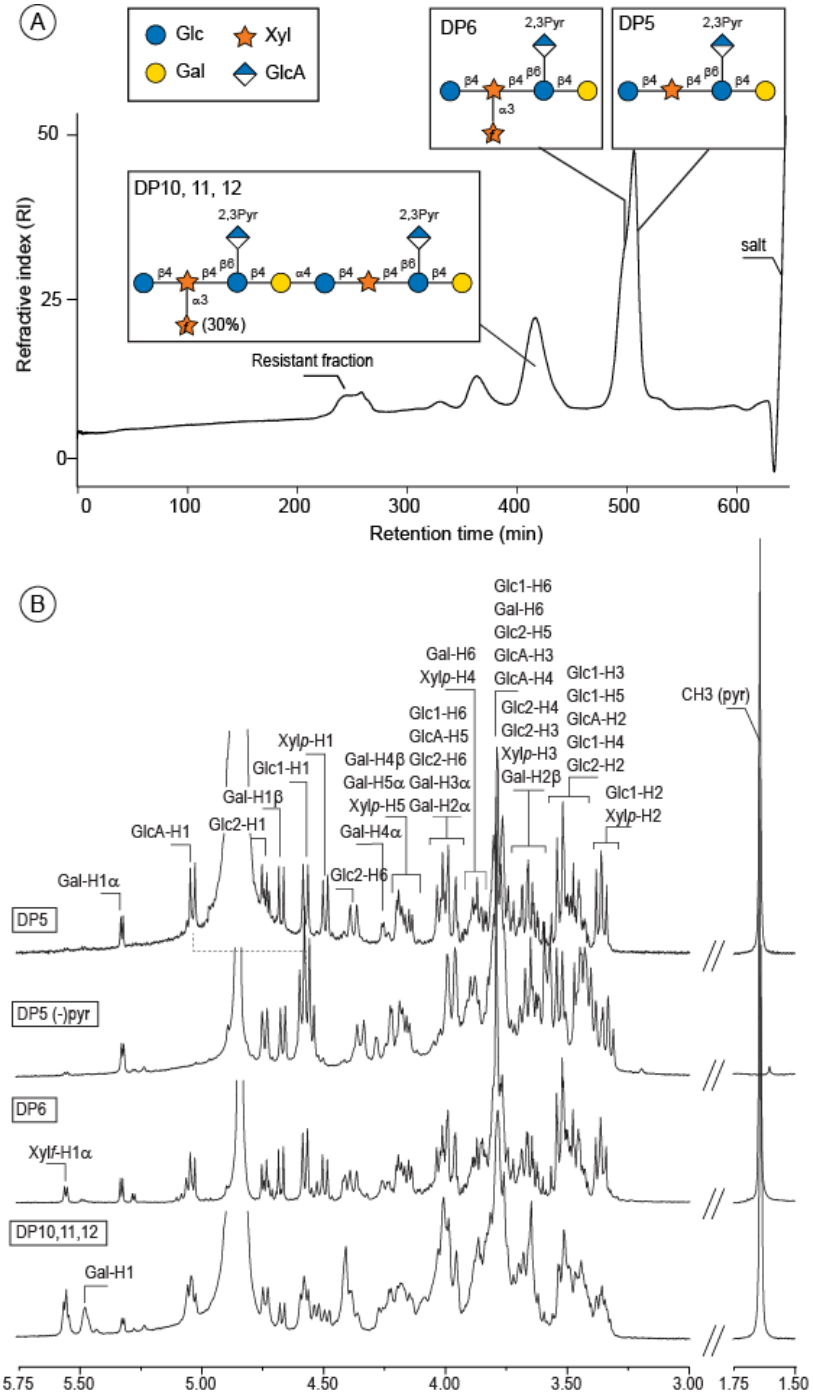

Figure 2. Purification and characterization of the enzymatic degradation products of *N. commune* polysaccharide. **A**) Size exclusion chromatography of the degradation products. Inset: the structure of the oligosaccharides determined by NMR analyses. **B**) ^{1}H NMR spectra of the oligosaccharides isolated after purification by chromatography. The spectra were recorded at 293 K

Table 3: ^{1}H and ^{13}C NMR chemical shifts of the oligosaccharides obtained after enzymatic degradation of the *N. commune* polysaccharide. Only the chemical shifts of the DP6 and longer oligosaccharides which were different from those of DP5 and depyruvated DP5 were reported in the table. [a]: Glc2→Galα / Glc2→Galβ values.

Sugar Residue		1	2	3	4	5	6 (6a,6b)	pyr (CH_3, C, CO)
DP5								
Glc-1 β-D-Glc*p*-(1→	^{1}H	4.57	3.36	3.53	3.47	3.52	3.98, 3.78	
	^{13}C	101.07	72.79	75.41	69.58	75.90	60.70	
Xylp →4)-β-D-Xyl*p*-(1→	^{1}H	4.49	3.36	3.65	3.88	4.16, 3.49		
	^{13}C	103.06	73.08	73.64	76.20	62.88		
Glc-2 →4,6)-β-D-Glc*p*-(1→	^{1}H	4.74/4.73[a]	3.44	3.66	3.72	3.73	4.37, 4.01	
	^{13}C	103.35/103.49 [a]	73.45	74.06	77.99	73.48	68.07	
Pyr-GlcA β-D-(2,3Pyr)-Glc*p*A-(1→	^{1}H	5.03	3.52	3.76	3.76	4.01	no	1.64
	^{13}C	101.29	75.59	80.72	78.47	70.57	175.33	22.56, 108.94, 175.99
Galα →4)-α-D-Gal*p*	^{1}H	5.32	3.95	4.01	4.26	4.19	3.87, 3.77	
	^{13}C	92.27	68.69	69.58	78.47	69.96	61.15	
Galβ →4)-β-D-Gal*p*	^{1}H	4.67	3.62	3.82	4.19	3.79	3.87, 3.77	
	^{13}C	96.38	72.07	73.16	77.25	74.47	61.29	
Depyruvated DP5								
Glc-1 β-D-Glc*p*-(1→	^{1}H	4.59	3.34	3.54	3.47	3.52	3.98, 3.78	
	^{13}C	101.09	72.78	75.48	69.55	75.93	60.67	
Xylp →4)-β-D-Xyl*p*-(1→	^{1}H	4.55	3.39	3.65	3.90	4.17, 3.44		
	^{13}C	102.91	73.01	73.74	76.40	62.87		
Glc-2 →4,6)-β-D-Glc*p*-(1→	^{1}H	4.75	3.44	3.66	3.77	3.73	4.35, 3.98	
	^{13}C	103.50/103.59 [a]	73.47	74.06	77.86	73.47	67.95	
GlcA β-D-Glc*p*A-(1→	^{1}H	4.57	3.42	3.56	3.52	3.77	no	
	^{13}C	102.63	72.83	75.48	71.82	76.33	175.81	
Galα →4)-α-D-Gal*p*	^{1}H	5.33	3.94	4.01	4.29	4.19	3.88, 3.78	
	^{13}C	92.28	68.70	69.55	78.44	69.84	60.92	
Galβ →4)-β-D-Gal*p*	^{1}H	4.67	3.62	3.82	4.23	3.79	3.88, 3.78	
	^{13}C	96.39	72.10	73.17	77.36	74.31	61.10	
DP6								
Xylp →3,4)-β-D-Xyl*p*-(1→	^{1}H	4.54	3.44	3.82	3.88	4.16, 3.49		
	^{13}C	103.02	72.26	79.87	76.20	62.68		
Xylf α-D-Xyl*f*-(1→	^{1}H	5.55	4.23	4.40	4.40	3.82		
	^{13}C	101.88	76.87	74.90	78.47	60.54		
DP10, 11, 12								
Glc-1 →4)-β-D-Glc*p*-(1→	^{1}H	4.59	3.39	3.81	3.70	3.64	3.98, 3.78	
	^{13}C	100.88	72.80	76.00	76.87	74.91	60.68	
Gal →4)-α-D-Gal*p*-(1→	^{1}H	5.47	4.00	4.01	4.22	4.11	3.87, 3.77	
	^{13}C	99.80	68.88	69.72	78.07	71.16	61.04	

221

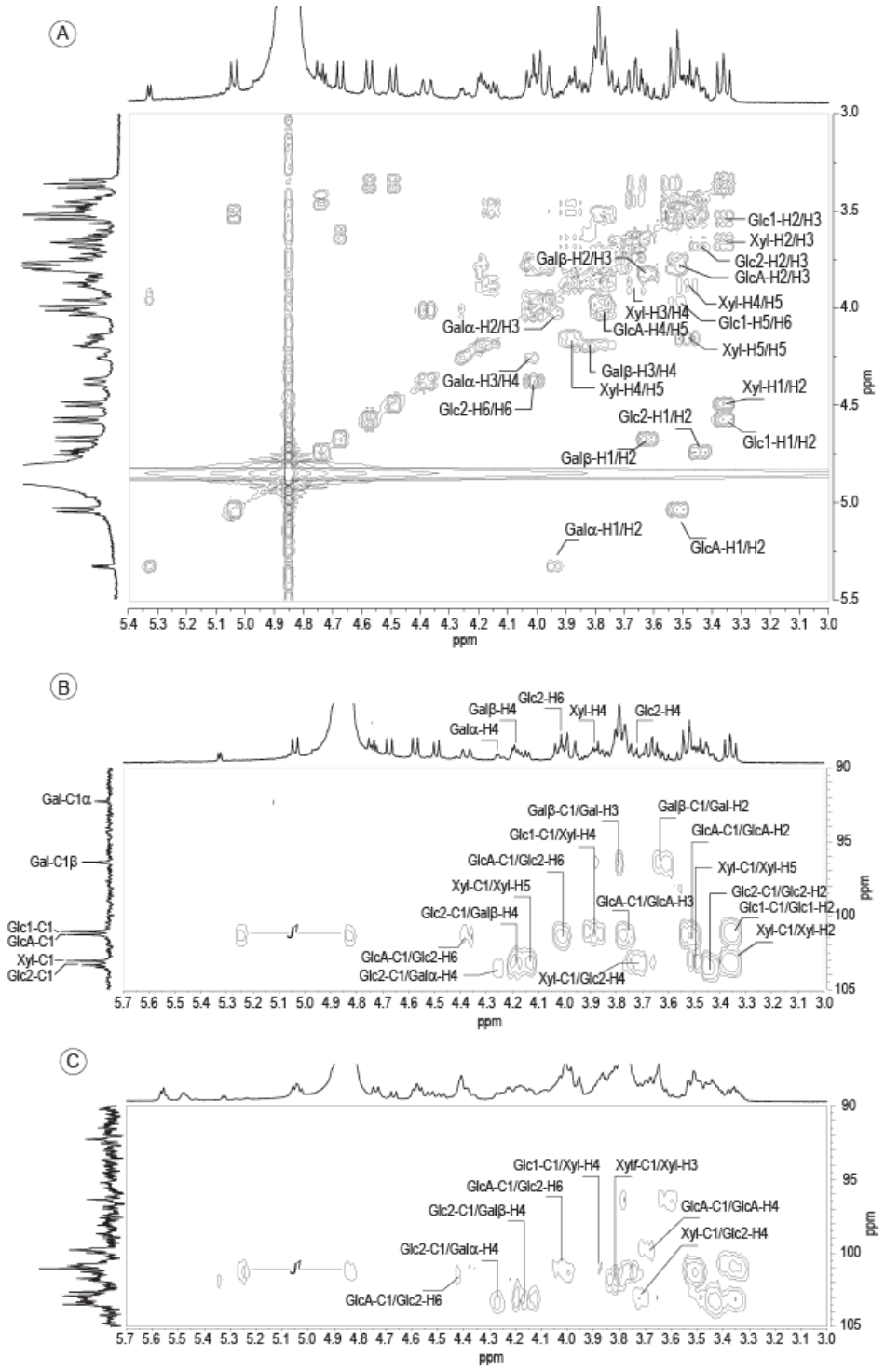

Figure 3. Analyses of the oligosaccharides by NMR. A) COSY spectrum of DP5. B) Detail of the HMBC spectrum of DP5. C) Detail of the HMBC spectrum of DP10, 11, 12. The spectra were recorded at 293 K.

222

Enzymatic degradation of the polysaccharide was monitored by size exclusion chromatography and oligosaccharides obtained after complete digestion of the macromolecule were collected (Figure 2A). Composition of the oligosaccharide fractions was determined (Figure S5) and their structure characterized by NMR (Figure 2B). The peak eluting at 507 min contained two oligosaccharides which could be identified by collecting different fractions of this peak. Based on composition analyses, ^{13}C and ^{1}H NMR spectra, the smallest oligosaccharide was found to have a degree of polymerization of DP=5 (elution time 510 min) with galactose at the reducing end and glucose at the non-reducing end as expected.

After mild acid hydrolysis, allowing the removal of the pyruvate group, the chemical shift of the glucuronic acid residue was shifted from C1/H1: 101.29/5.03 ppm to C1/H1; 102.63/4.57 ppm (Figure 2B, spectra DP5(-)Pyr). Analysis of the correlation system in the COSY (Figure 3A) allowed attributing the chemical shifts to five residues: the galactose located at the reducing end (Galα-C1/H1: 92.27/5.32 ppm and Galβ-C1/H1: 96.38/4.67 ppm), the glucose residue at the non-reducing end (Glc1nr-C1/H1: 101.07/4.57 ppm), the glucuronic acid residue decorated by a pyruvate (GlcA-C1/H1: 101.29/5.03 ppm), a second glucose residue (Glc2-C1/H1→Galα: 103.35/4.74 ppm and Glc2-C1/H1→Galβ: 103.49/4.73 ppm) and a xylopyranoside residue (Xyl-C1/H1: 103.06/4.49ppm) (Table 3). The linkage between these residues were determined straightforwardly using heteronuclear $^{1}H/^{13}C$ chemical shift correlation (HMBC, Figure 3B). Altogether the structure of the oligosaccharide deduced from these analyses was a pentasaccharide made of the tetrasaccharide: β-D-Glc (1 → 4)-β-D-Xyl (1 → 4)-β-D-Glc (1 → 4)-α/β-D-Gal, branched with a 2,3pyruvated β-D-GlcA linked at the position 6 of the internal glucose residue.

We noticed that the two glucose residues observed in the main chain presented very different chemical shifts. The residue Glc1nr-C1/H1: 101.07/4.57 ppm showed a lower C1/H1 chemical shifts than for the residue Glc2 (Glc2-C1/H1→Galα: 103.65/4.74 ppm and Glc2-C1/H1→Galβ: 103.49/4.73 ppm). The resolution of the NMR spectra recorded on the oligosaccharides and, more especially, the carbon/proton coupling observed in heteronuclear single quantum coherence (HSQC) were obvious. The lower Glc1-C1/H1 chemical shifts is explained by its bounding to a xylose residue as previously observed by Helm and co-workers (2000). Calculating of the chemical shifts using the online CASPER program (http://www.casper.organ.su.se/casper/; Lundborg and Widmalm, 2011) gave Glc1-C1/H1= 101.94/4.59 ppm and Glc2-C1/H1 = 104.48/4.65 ppm which values were close to those recorded.

The asymmetric center of the pyruvate group was determined by NOESY (Nuclear Overhauser Effect Spectroscopy) according to the same strategy reported by Severn & Richards (1992). The NOESY spectrum revealed a long distance correlation between the protons of the methyl group of pyruvate (Pyr-CH3= 1.64 ppm) with proton H2 of the glucuronic residues (GlcA-H2=3.52 ppm). No correlation was observed with proton H3 demonstrating the pyruvate group adopted the R configuration.

Composition analyses of the fractions containing higher size oligosaccharides were enriched in xylose residues (Figure S5) suggesting the branching of xylose residues on the main chain as observed for the undigested polysaccharide. The fraction collected at 495 min, contained an oligosaccharide which NMR spectra and chemical shifts recorded in ^{1}H and ^{13}C were almost identical to that of the previous DP5 suggesting a very similar structure (Figure 2B, DP6). However, additional signals observed in NMR spectra (Xylf-C1 =101.88 ppm, Xylf-H1 = 5.55 ppm were attributed to an additional residue suggesting the occurrence of an oligosaccharide of DP=6. Comparison and of the DP5 and DP6 spectra, as well as the proton correlation system evidenced by the well-resolved COSY spectra and the $^{1}H/^{13}C$ chemical shift correlation highlighted by the HMBC spectra allowed determining straightforwardly the chemical shifts and the coupling constants. The data recorded were in agreement with an α-xylofuranoside residue and similar to interpretations reported in previous works (Angyal, 1979; Kocharova et al., 1994). Other furanoside residues not detected in composition analyses could also be excluded after NMR investigations. Indeed, the expected C4/H4= 84.7 ppm/4.11 ppm of α-ribofuranose (Helm et al., 2000), the H4 = 3.68 ppm of α-mannofuranose (Angyal, 1979) or C4/H4= 82 ppm /3.71 ppm of α-galactofuranoside (Katzenellenbogen et al. 2012) were too different to the recorded C4/H4 = 78.47 ppm/4.40 ppm attributed to the α-xylofuranoside. Signals of the heteronuclear $^{1}H/^{13}C$ chemical shift correlation (HMBC) were too weak to determine unambiguously the linkage of the residue.

The peak eluting at 415 min was a mixture of several oligosaccharides which were not isolated and which sizes were estimated to DP10, 11 or 12, corresponding to different combinations of the DP5 and DP6. Based on the signal attribution of the DP5 and DP6, most of the ^{1}H and ^{13}C NMR signals could be ascribed (Table 3). More interestingly, the linkage between the Glc and Gal residues cleaved by the enzymes was determined using heteronuclear $^{1}H/^{13}C$ chemical shift correlation (HMBC, Figure 3C). The correlation between the Gal-C1 and Glc-H4 observed in the spectrum, demonstrated unambiguously the α-D-Gal (1→4)-D-Glc linkage. The linkage of the xylofuranoside residue was also well identified in the HMBC spectra and revealed the residue was bound to the xylopyranoside residue of the main chain by (1,3) linkage. The repeating unit of the polysaccharide deduced from the detailed analyses of the oligosaccharide and the the unmodified polymer was:

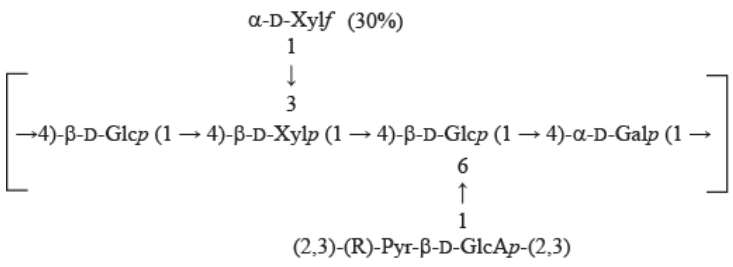

3.4 Dispersion and diversity of Nostoc commune polysaccharides

After an exhaustive survey of the literature, the structures of the polysaccharides secreted by Nostoc strain were presented in Figure 4. The polysaccharide secreted by the *Nostoc* strain isolated at Saint Martin d'Uriage (France, Europe) showed very similar structural characteristic with those secreted by several Asian strains (Figure 4). The polysaccharide of *Nostoc commune* strains isolated in Mongolia, China or Japan shared a tetra-saccharide repeating unit:[→ 4) β-D-Glc (1 → 4)-β-D-Xyl (1 → 4)-β-D-Glc (1 → 4)-α-D-Gal (1 →], systematically branched at position 6 of a glucose residue by a β-linked glucuronic acid residue. No decoration of the glucuronic acid residue was reported for the polysaccharide secreted by the Chinese strain (Brüll et al., 2000). A lactate group was observed in the case of the polysaccharide of the Mongolian origin (Helm et al., 2000) instead of the pyruvate group found in our studied polysaccharide. Interestingly, both lactate and pyruvate were identified in the polysaccharides of a strain isolated in Japan (Kajiyama et al., 2001) suggesting that derivatization of the glucuronic acid residue by lactate or pyruvate can co-occur in *Nostoc commune*. The occurrence of only one specific group - pyruvate or lactate - may reflect some adaptation to the environment or are an independent evolution of the strains which could have abandoned one derivatization pathway. Also it can't be excluded that specific modification of the polysaccharides may be caused by biotic interactions such as, for example, co-existing bacterial strains.

Another difference observed is the replacement of the ribose residue found in the Mongolian strain polysaccharide by a xylose residue in our study, adopting in both cases the furano configuration. In a biosynthesis point of view, the replacement a D-ribose by L-xylose its epimer at position 3 residue is not biochemically improbable and could proceed from an evolution of the biosynthetic pathway. Composition analyses of polysaccharides secreted by various strains of *N. commune* show that in addition to ribose and xylose, other residues such as arabinose, fucose or rhamnose could occur along the polysaccharide chain (Huang, Liu, Paulsen & Klaveness 1998; De Philippis, Ena, Paperi, Sili & Vincenzini, 2000). Altogether, its seems that the polysaccharides secreted by *Nostoc commune* strains isolated in various place in the world have conserved structural characteristic which suggested a selection pressure on the biosynthetic pathway leading to the preservation of mandatory biological and physico-chemical properties. The capacity of the gelatinous substance embedding of the cyanobacterial cells composed of the polysaccharide, associated to another component such as proteins, is probably its capacity to swell/de-swell as a function of the amount of water in a reversible way. Implication of the polysaccharide in the defence mechanisms as a mechanical or biological barrier to protect akinete resting cells probably played also a role in maintaining the structural properties of the polysaccharide.

N. commune strain investigated in this study and the strains isolated in the desert of Mongolia (*N. commune* DRH-1) were identified using genetic tools. Few other structural data on the polysaccharides

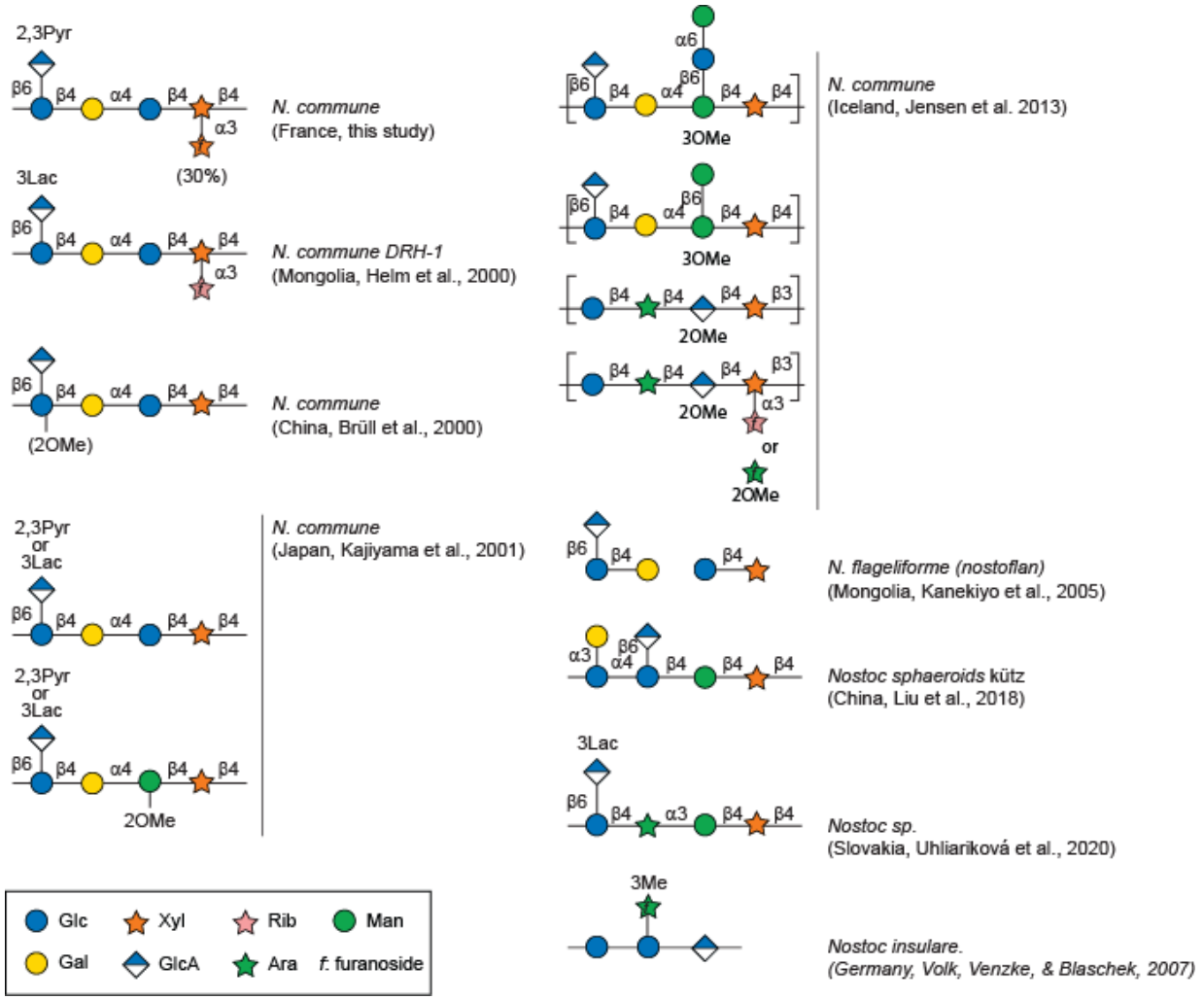

Figure 4. Comparison of the structures of the polysaccharides secreted by *Nostoc* sp. strains isolated in various places in the world.

secreted by other species of *Nostoc* were also reported. However, genetic data were lacking and identification of the species was based on morphology considerations. In this context, comparison of the polysaccharide structures in regard to the evolution of *Nostoc* species is therefore difficult. However, the oligosaccharides obtained after acid hydrolysis of the polysaccharide of a strain identified as *Nostoc flagelliforme* (Mongolia, Kanekiyo et al., 2005) suggested also a conserved carbohydrate backbone with the same pentasaccharide sequence. *Nostoc commune* can form filament depending on growth condition and it is then difficult to discriminate some *Nostoc commune var flagelliforme* with true *Nostoc flagelliforme*. Structure of reported *Nostoc sp.* polysaccharides presented in Figure 4 suggested that the repeating unit made of a penta-saccharide seemed common probably reflecting a common biosynthesis template which evolved in the *Nostoc* lineages.

4. Conclusion

The structure of the polysaccharide secreted by the strain of *N. commune* isolated in Saint Martin d'Uriage (France) was resolved. Comparison of our results with previously characterized structure of polysaccharide of *N. commune* strains found in Europe and Asia suggested the conservation of a pentasaccharide template reflecting a conservation of the biosynthesis pathway. The building block made of the tetrasaccharide [→4)-β-D-Glc (1→4)-β-D-Xyl (1→4)-β-D-Glc (1→4)-α-D-Gal (1→], systematically branched by a β-linked glucuronic acid, presented lactate and pyruvate derivatives according to the origin of the *Nostoc commune* strain. Also, we noticed that a mannose or methylated mannose glucose residue was found in place of a glucose residue of the main chain. The structure of *N. flageliforme* polysaccharides showed was similar to *N. commune* suggesting a common biosynthesis pathway ancestor. The important role of the polysaccharide in the growth and survival of the cyanobacterial cells supposes that strong alteration of modification of the structure and, therefore, the associated physico-chemical properties will be detrimental to the cells. The conservation of the polysaccharide structure of the world-wide spread *N. commune* strains probably reflects a strong selection pressure on the structure of the polysaccharides.

Acknowledgments

This work was supported by the French National Research Agency (Grant ANR-14-CE06-0017). W.H., E.M and A.A have received support from the Glyco@Alps Cross-Disciplinary Program (Grant ANR-15-IDEX-02), Labex ARCANE, and Grenoble Graduate School in Chemistry, Biology, and Health (Grant ANR-17-EURE-0003). E.M. and A.A. are supported by Grant Alpalga ANR-20-CE02-0020.

References

Angyal, S.J. (1979) Hudson's rules of isorotation as applied to furanosides, and the conformations of methyl aldofuranosides. *Carbohydrate Research, 77*, 37-50

Blakeney A.B., & Stone B.A. (1985) Methylation of carbohydrates with lithium methylsulphinyl carbanion. *Carbohydr. Res.* 140 319–324.

Boutte, C., Grubisic, S., Balthasart, P., & Wilmotte, A. (2006) Testing of primers for the study of cyanobacterial molecular diversity by DGGE. *Journal of Microbiological Methods*, *65*, 542-550

Brüll, L.P., Huang, Z., Thomas-Oates, J.E., Paulsen, B.S., Cohen, E.H., & Michaelsen, T. E. (2000) Studies of polysaccharides from three edible species of Nostoc (cyanobacteria) with different colony morphologies: structural characterization and effect on the complement system of polysaccharides from *Nostoc commune*. *Journal of Phycology, 36*, 871–881

Davey, M.C. (1989) The effects of freezing and desiccation on photosynthesis and survival of terrestrial antarctic algae and cyanobacteria. *Polar Biology, 10*, 29-36

De Philippis, R., Ena, A., Paperi, R., Sili, C., & Vincenzini, M. (2000) Assessment of the potential of *Nostoc* strains from the Pasteur culture collection for the production of polysaccharides of applied interest. *Journal of Applied Phycology, 12*, 401–407

Dodds, W.K., & Gudder, D.A. (1995) The ecology of Nostoc. *Journal of Phycology, 31*, 2-18

Fleming, E.D., & Prufert-Bebout, L. (2010) Characterization of cyanobacterial communities from high-elevation lakes in the Bolivian Andes: high-elevation Andes Cyanobacteria. *Journal of Geophysical Research, 115*, G00D07, doi:10.1029/2008JG000817

Gao, K. (1998) Chinese studies on the edible bluegreen alga, *Nostoc flagelliforme*: a review. *Journal of Applied Phycology, 10*, 37–49

Hakomori, S.I. (1964) A rapid permethylation of glycolipid, and polysaccharide catalyzed by methylsulfinyl carbanion in dimethyl sulfoxide. *Journal of Biochemistry, 55*, 205–208.

Hall, T.A. (1999) BioEdit: a user-friendly biological sequence alignment editor and analysis program for Windows 95/98/NT. *Nucleic Acids. Symposium series, 41*, 95-98.

Helbert, W., Poulet, L., Drouillard, S., Mathieu, S., Loiodice, M., Couturier, M., Lombard, V., Terrapon, N., Turchetto, J., Vincentelli, R. & Henrissat, B. (2019) Discovery of novel carbohydrate-active enzymes through the rational exploration of the protein sequences space. *Proceeding of National Academy of Sciences, 116*, 6063-6068

Helm, R. F., Huang, Z., Edwards, D., Leeson, H., Peery, W., & Potts, M. (2000) Structural Characterization of the Released Polysaccharide of Desiccation-Tolerant Nostoc commune DRH-1. *Journal of bacteriology, 182*, 974-982

Hu, C., Liu, Y., Paulsen, B.S., Petersen, D., Klaveness, D. (2003) Extracellular carbohydrate polymers from five desert soil algae with different cohesion in the stabilization of fine sand grain. *Carbohydrate Polymers, 54*, 33-42

Huang, Z, Liu, Y., Paulsen, B.S., & Klaveness, D. (1998) Studies on polysaccharides from three edible species of Nostoc (cyanobacteria) with different colony morphologies: comparison of monosaccharide compositions and viscosities of polysaccharides from field colonies and suspension cultures. *Journal of Phycology, 34*, 962–968

Jensen, S., Petersen, B.O., Omarsdottir, S., Paulsen, B.S., Duus ,J.Ø., & Olafsdottir, E.S. (2013) Structural characterisation of a complex heteroglycan from the cyanobacterium *Nostoc commune*. *Carbohydrate Polymers, 91*, 370-376

Kajiyama, S., Yagi, M., Kurihara, T., Okazawa, A., Fukusaki, E.-I., & Kobayashi, A. (2001) Structure of hetero polysaccharide from desiccation-tolerant terrestrial cyanobacterium *Nostoc commune*. *Symposium on the Chemistry of Natural Products, symposium papers, 43*, 193-198.

Kamerling, J.P., Gerwig, G.J., Vliegenthart, J.F., & Clamp, J.R. (1975) Characterization by gas-liquid chromatography mass spectrometry and proton-magnetic-resonance spectroscopy of pertrimethylsilyl methyl glycosides obtained in the methanolysis of glycoproteins and glycopeptides. *Biochemical Journal, 151*, 491–495.

Kanekiyo, K., Lee, J.-B., Hayashi, K., Takenaka, H., Hayakawa, Y., Endo, S., & Hayashi, T. (2005) Isolation of an antiviral polysaccharide, nostoflan, from a terrestrial cyanobacterium, *Nostoc flagelliforme*. *Journal of Natural Products, 68*, 1037-1041

Katzenellenbogen, E, Kocharova N.A., Górska-Frączek, S., Gamian, A., Shashkov A.S. & Knirel Y.A. Structural and serological studies on the O-antigen show that *Citrobacter youngae* PCM1505 must be classified to a new Citrobacter O-serogroup. *Carbohydrate Research, 2012,* 360, 52-55

Kocharova, N.A., Knirel, Y.A., Shashkov, A. S., Kochetkov, N. K., Kholodkova, E. V., & Stanislavsky E. S. (1994) The structure of the *Citrobacter freundii* O8a,8b O-specific polysaccharide containing D-xylofuranose. *Carbohydrate Research, 263,* 327-331

Kvernheim A.L. (1987) Methylation analysis of polysaccharides with butyllithium in dimethyl sulfoxide. *Acta Chem. Scand*. B41 150–152.

Kvernheim, A.L. (1987) Methylation analysis of polysaccharides with butyllithium in dimethyl sulfoxide. *Acta Chemica Scandinavica B, 41*, 150–152.

Linnerborg M., Wollin R. and Widmalm G. (1997*). Structural Studies of the O-Antigenic Polysaccharide from* Escherichia Coli *O167* Eur J Biochem. 246, 565-73.

Liu, Y., Su, P., Xu, J., Chen, S., Zhang, J., Zhou, S., Wang, Y., Tang, Q., & Wang Y. (2018) Structural characterization of a bioactive water-soluble heteropolysaccharide from *Nostoc sphaeroids* kütz. *Carbohydrate Polymers, 200*, 552-559

Lundborg, M., and Widmalm, G. (2011) Structure Analysis of Glycans by NMR Chemical Shift Prediction. *Anal. Chem., 83,* 1514-1517. Doi: 10.1021/ac1032534.

Montreuil, J., Bouquelet, S., Debray, H., Fournet, B., Spik, G., & Strecker, G. (1986) Glycoproteines. In *Carbohydrates Analysis: A Practical Approach* (pp. 143–204). Chaplin, M.F., Kennedy, J.K., Eds.; IRL Press: Oxford, UK,

Novis, P., Whitehead, D., Gregorich, E.D.G., Hunt, J., Sparrow, A.D., Hopkins, D.W., Elberling, B. & Greenfield, L.G. (2007) Annual carbon fixation in terrestrial populations of *Nostoc commune* (Cyanobacteria) from an Antarctic dry valley is driven by temperature regime. *Global Change Biology, 13,* 1224–1237

Pereira, S., Zille, A., Micheletti, E., Moradas-Ferreira, P., De Philippis, R., & Tamagnini, P. (2009) Complexity of cyanobacterial exopolysaccharides: composition, structures, inducing factors and putative genes involved in their biosynthesis and assembly. *FEMS microbiology reviews, 33,* 917–941

Perez, R., Forchhammer, K., Salerno, G. & Maldener, I. (2016) Clear differences in metabolic and morphological adaptations of akinetes of two Nostocales living in different habitats. *Microbiology, 162,* 214–223

Qui, B., Liu, J., Liu, Z., & Liu, S. (2002) Distribution and ecology of the edible cyanobacterium Ge-Xian-Mi (Nostoc) in rice fields of Hefeng County in China. *Journal of Applied Phycology, 14,* 423–429.

Sand-Jensen, K. (2014) Ecophysiology of gelatinous Nostoc colonies: unprecedented slow growth and survival in resource-poor and harsh environments. *Annals of Botany, 114,* 17–33

Severn, W.B. and Richards, J.C. (1992) The acidic specific capsular polysaccharide of *Rhodococcusequi* serotype-3 - structural elucidation and stereochemical analysis of the lactate ether and pyruvate acetal substituents. *Canadian Journal of Chemistry, 70,* 2664-2676.

Taylor, R.L., & Conrad, H.E. (1972) Stoichiometric depolymerization of polyuronides and glycosaminoglycans to monosaccharides following reduction of their carbodiimide activated carboxyl groups. *Biochemistry, 11,* 1383–1388.

Uhliariková, I., Šutovská, M., Barboríková, J., Molitorisová, M., Kim, H.J., Park, Y.I., Matulová, M., Lukavský, J., Hromadková, Z., & Capek, P. (2020) Structural characteristics and biological effects of exopolysaccharide produced by cyanobacterium *Nostoc sp*. *International Journal of Biological Macromolecules, 160,* 364-371

Volk, R.B., Venzke, K., & Blaschek, W. (2007) Structural investigation of a polysaccharide released by the cyanobacterium *Nostoc insulare*. *Journal of Applied Phycology*, *19*, 255-262.

Supporting information

Supplementary Figures

Figure S1: Gas chromatogram recorded on the hydrolysis products of the *Nostoc commune* polysaccharide. Inset: Molar ratio of the various detected residues.

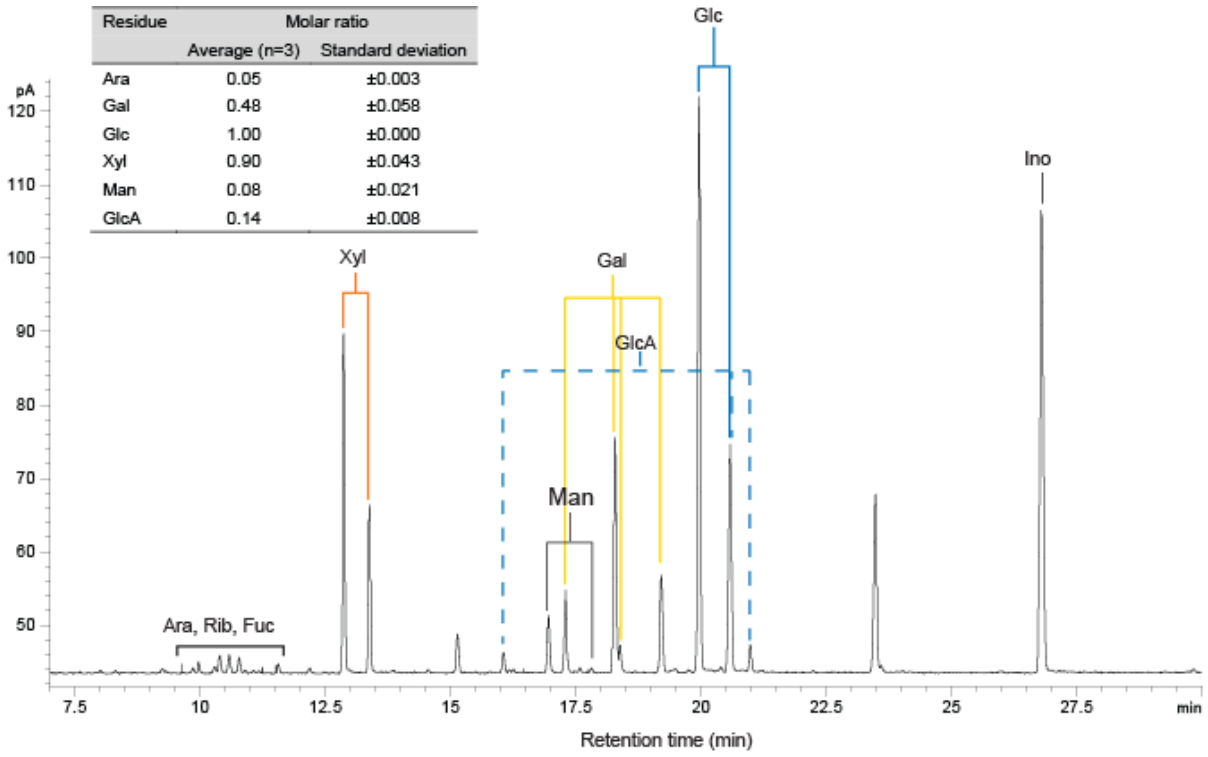

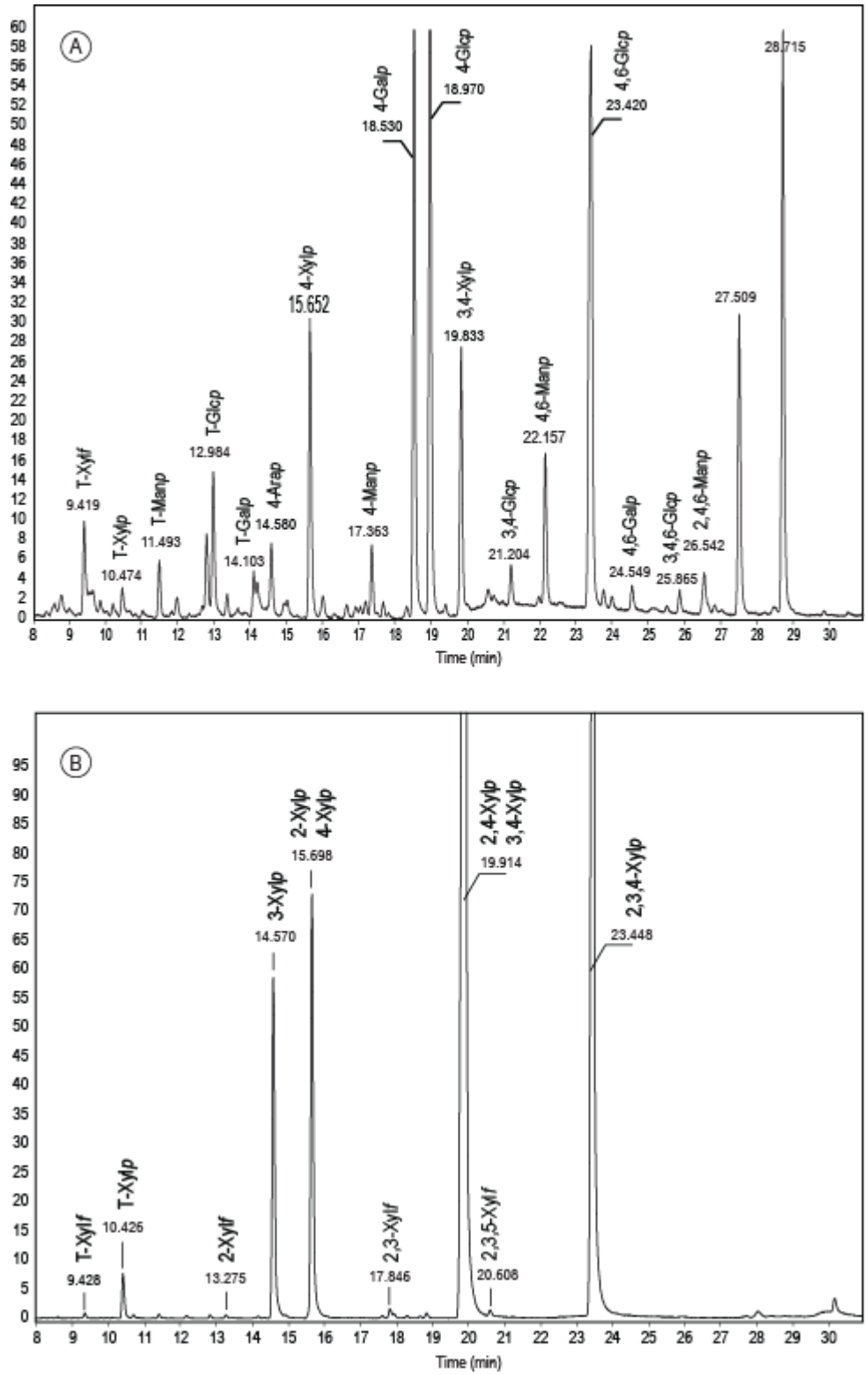

Figure S2: Gas chromatogram recorded on the permethylated residues of the *Nostoc commune* polysaccharide (**A**) and the xylose standard residues (**B**).

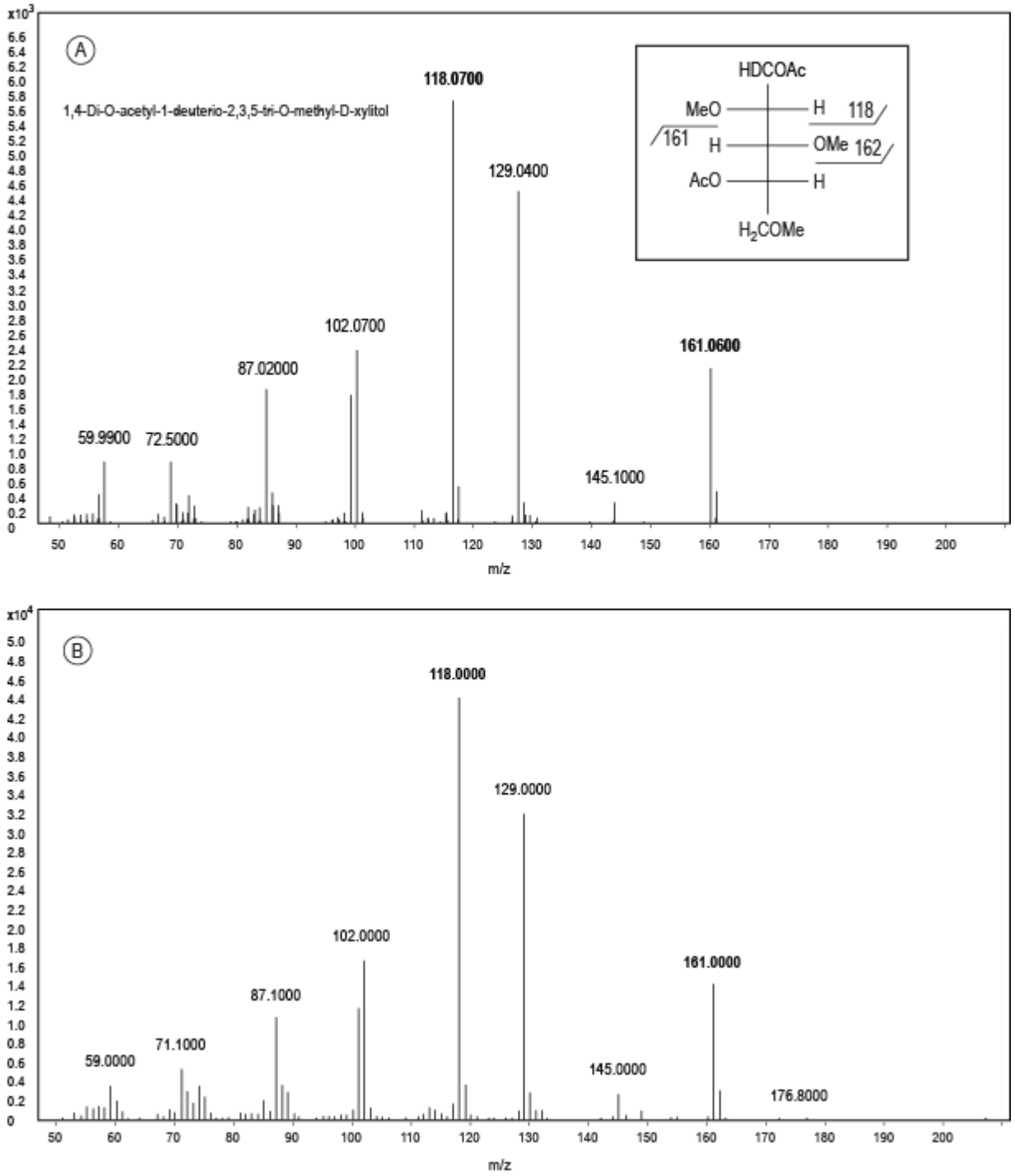

Figure S3: (A) Fragmentation product of the 1,4-di-O-acetyl-1-deuterio-2,3,5-tri-O-methyl-D-xylitol eluting at 9.468 min in the gas chromatogram of the xylose derivatives standard (Figure S3A). **(B)** Fragmentation products obtained on the derivatives eluting at 9.419 in the gas chromatogram recorded on the *N. commune* polysaccharide (Figure S3B)

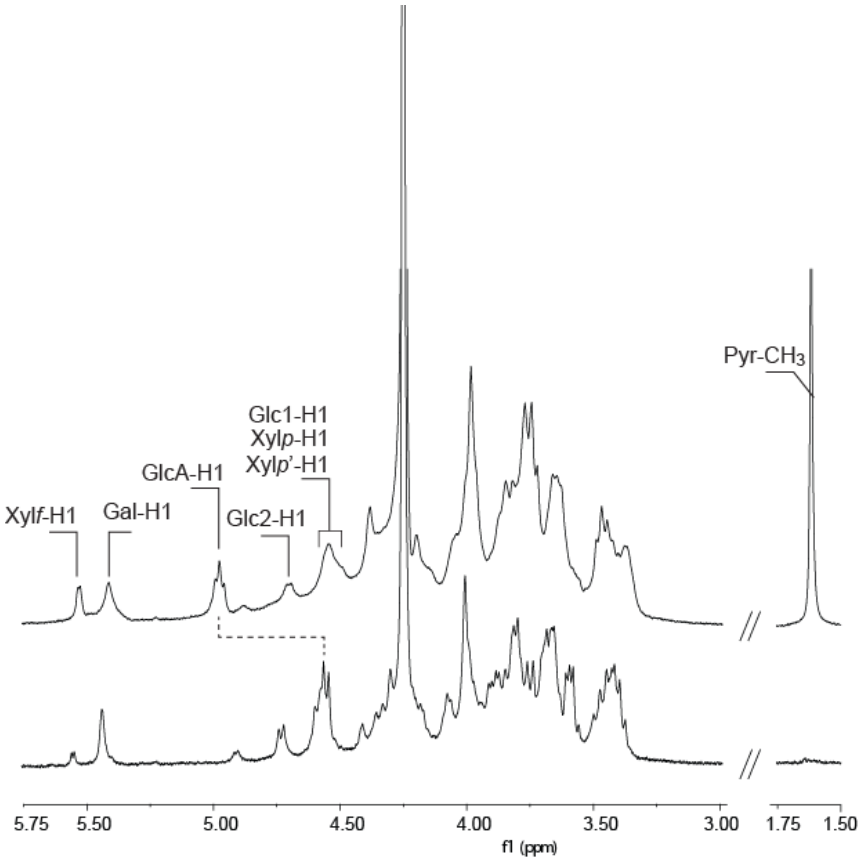

Figure S4. ^{1}H NMR spectra of the *Nostoc commune* polysaccharides. Top: The purified polysaccharide. Bottom: The polysaccharide was subjected to mild acid treatment. The spectra were recorded at 353 K

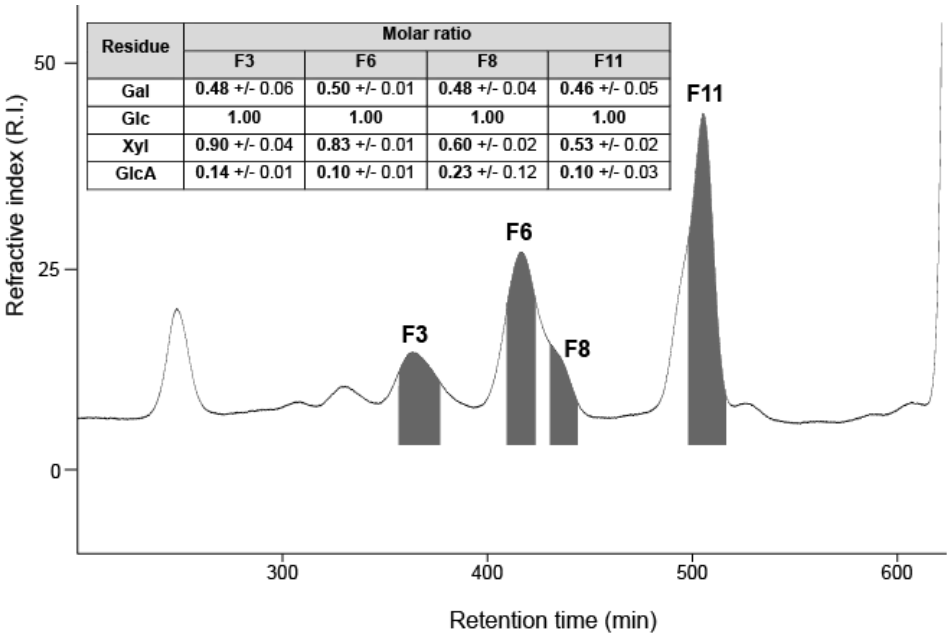

Figure S5: Size exclusion chromatogram recorded on the enzymatic degradation products of *N. commune* polysaccharide. The composition of the oligosaccharides collected were determined and reported in the inserted table.